Kinetic Mechanism of Human Histone Acetyltransferase P/CAF†

Kirk G. Tanner, Michael R. Langer, and John M. Denu*

Department of Biochemistry and Molecular Biology, Oregon Health Sciences University, Portland, Oregon 97201-3098

Received June 2, 2000; Revised Manuscript Received August 2, 2000

ABSTRACT: Human transcriptional coactivator P/CAF (*p*300/*C*BP-*a*ssociating *f*actor) is a histone acetyltransferase (HAT) and is a member of the GNAT (GCN5 related *N*-acetyltransferases) superfamily. P/CAF was originally identified by its ability to activate transcription of a variety of genes through its interaction with p300/CBP. Though Lys-14 of histone H3 appears to be the preferred substrate, other nonhistone proteins can also serve as substrates for P/CAF. However, few studies have addressed the catalytic and kinetic mechanisms of histone/protein acetylation by P/CAF. In this study, we have systematically determined the kinetic mechanism for P/CAF, identified the critical ionizations for binding/catalysis, and established the rate-limiting step in turnover. This was accomplished by a variety of approaches including pH-dependent activity measurements, Bi-substrate kinetic analysis, authentic product inhibition by coenzyme A (CoA) and acetylated H3 (Ac-Lys-14) peptide, direct measurements of substrate/product binding affinities (equilibrium dialysis), and a pre-steady-state quench-flow analysis. The results are consistent with a fully ordered Bi-Bi kinetic mechanism, where chemical catalysis is rate-determining. Acetyl-CoA (AcCoA) binds with high affinity ($K_d = 0.64 \pm 0.12$ μM) to the free form of the enzyme. Histone H3 peptide binds (apparent $K_d = 116 \pm 17$ μM) only after AcCoA is bound. No H3 peptide binding to the free enzyme was detectable. In the ternary complex, the ϵ-amino of Lys-14 (H3 peptide substrate) directly attacks the carbonyl carbon of AcCoA, transferring the acetyl group to the acceptor peptide substrate (rate-limiting step). Products are released in an ordered fashion, with Ac-Lys-14 H3 released first followed by release of CoA. The pH dependency of the k_{cat}/K_m parameter revealed two P/CAF ionizable groups (pK_a values of 6.9 and 7.5) that must be unprotonated for activity. The group with a pK_a value 7.5 was assigned to Glu-570, which is the proposed general base catalyst, abstracting a proton from the ϵ-amino group and facilitating nucleophilic attack.

The human transcriptional coactivator P/CAF[1] (*p*300/*C*BP-*a*ssociating *f*actor) is a member of the GNAT (GCN5 related *N*-acetyltransferases) superfamily (*1*) and has intrinsic histone acetyltransferase (HAT)[1] activity (*2*). Although several gene families of HATs have been identified (*3, 4*), the GCN5 family has been the most characterized. Within the GCN5 HAT domain, the putative HAT domain of P/CAF shares 43% sequence identity, suggesting an evolutionarily conserved catalytic mechanism. P/CAF was originally identified by its ability to activate the transcription of a variety of genes through its interaction with p300/CBP (*2, 5, 6*). P/CAF was also shown to counteract the inhibitory effects of the adenoviral E1A oncoprotein on p300/CBP-mediated transcriptional activation (*2*). P/CAF is now recognized as an important factor in the chromatin remodeling process by directly acetylating histone H3 and histone H4 within the nucleosome.

Though P/CAF has been shown to acetylate a variety of substrates including nonhistone proteins, the preferred histone substrate is Lys-14 of histone H3 and to a lesser extent Lys-8 of histone H4 (*7*). P/CAF has been shown to acetylate the nonhistone proteins myo-D (*8*), TFIIEβ (Lys-52), HMG-17 (Lys-2) (*9*), and p53 (Lys-320) (*10*). In vivo, the chromatin remodeling effects of P/CAF are exerted in the context of a large complex with the master regulator of transcription CBP/p300 (*4*).

Full-length P/CAF is a 90 kDa, 832 residue protein that contains 2 well-defined domains and an N-terminal sequence that demonstrates homology with mammalian GCN5 and is required for interaction with p300/CBP (*11*). The C-terminal domain of P/CAF has been identified as a bromo domain which is found in many transcriptional effectors (such as CBP/p300). A recent nuclear magnetic resonance (NMR)[1] solution structure of the bromo domain of P/CAF has revealed that this domain adopts a fold that can interact specifically with acetylated lysine (*12*), thus functionally coupling the bromo domain with the HAT activity of coactivators in the regulation of gene transcription. The other well-defined domain is the central HAT domain which displays a high degree of sequence homology to the GCN5 transcriptional coactivator from *Tetrahymena* and yeast (*13*). Recently, the crystallographic molecular model of a binary complex of the P/CAF HAT domain (residues 493−658) and

† J.M.D. was supported by American Cancer Society Grant RPG-97-175-01-TBE and NIH Grant GM 59785-01 and K.G.T. by Postdoctoral Fellowship T32 DK07680.

* Correspondence should be addressed to this author at the Department of Biochemistry and Molecular Biology, Oregon Health Sciences University, 3181 SW Sam Jackson Park Rd., Portland, OR 97201-3098. Phone: (503) 494-0644. Fax: (503) 494-8393. Email: denuj@ohsu.edu.

[1] Abbreviations: HATs, histone acetyltransferases; P/CAF, (*p*300/*C*BP-*a*ssociating *f*actor); AcCoA, acetyl-coenzyme A; CoA, coenzyme A; Ac-Lys-14, acetyl-Lys-14; DTT, dithiothreitol; mbB, monobromobimane; NMR, nuclear magnetic resonance.

10.1021/bi001272h CCC: $19.00
Published on Web 09/07/2000

coenzyme A (CoA) has been solved by Marmorstein and colleagues (*14*). In this structure, CoA is bound in a pronounced cleft that is roughly orthogonal to second larger cleft which is thought to be the site of histone substrate binding. Consistent with this notion, the X-ray structure of *Tetrahymena* GCN5 bound to both an H3 peptide and CoA revealed that the H3 peptide can occupy the larger cleft (*15*). These structures demonstrated that the two orthogonal clefts converge near the ϵ-amino group of Lys-14 of histone H3 peptide and the sulfhydryl of CoA. A conserved acidic residue (Glu-173 in yeast GCN5, Glu-570 in P/CAF) is positioned near the site of convergence. We had previously established Glu-173 of yeast GCN5 to be a critical catalytic residue and demonstrated that this glutamic acid was acting as a general base catalyst, deprotonating the ϵ-amino of Lys-14 to facilitate attack at the carbonyl carbon of acetyl-coenzyme A (AcCoA) (*16*). Consistent with the resolved structures and our previous biochemical data, these reactions likely involve direct acetyl group transfer from AcCoA to the acceptor lysine residue in a enzyme ternary complex. However, direct evidence for the proposed catalytic and kinetic mechanism for P/CAF is lacking.

To better understand the biology of this important transcriptional coactivator, it will be necessary to elucidate the details of substrate selectivity and the molecular mechanism. In this study, we have systematically determined the kinetic mechanism for P/CAF, identified the critical ionizations for binding/catalysis, and established the rate-limiting step in turnover. This was accomplished by a variety of approaches including pH-dependent activity measurements, Bi-substrate kinetic analysis, product inhibition by CoA and acetylated (Ac-Lys-14) H3 peptide, direct measurements of substrate/product binding affinities (equilibrium dialysis), and a pre-steady-state quench-flow analysis. The results presented in the current study are consistent with a fully ordered sequential Bi-Bi kinetic mechanism, where chemical catalysis is rate-determining.

EXPERIMENTAL PROCEDURES

Materials. AcCoA was purchased from Boehringer Mannheim. Calf thymus histones were purchased from Calbiochem. [^{3}H]Acetyl-CoA (1.88 Ci/mmol) was from NEN Life Sciences Products. Histone H3 peptide, ARTKQTARKSTGGKAPPKQLC, and the Lys-14 acetylated H3 peptide (Ac-Lys-14),[1] corresponding to the 20 amino-terminal residues of human histone H3 and an additional carboxy-terminal cysteine, were synthesized by the Protein Chemistry Core Lab at The Baylor College of Medicine. Dispo-Equilibrium Dialyzers were from Amika Corp. P81 phosphocellulose disks were from Gibco Life Sciences. Monobromobimane (mbB)[1] was from Molecular Probes. All other reagents were of the highest grade available and were from either Fisher Scientific or Sigma Chemical Co.

Expression and Purification. The catalytic domain (amino acids 493−658) of human P/CAF was recombinantly expressed by isopropyl-β-D-thiogalactopyranoside (IPTG) induction for 12 h at 25 °C and purified from BL21-DE3 bacteria, similar to previously published methods (*17*). Harvested cells were lysed by French pressure in 50 mM Tris (pH 7.5), 150 mM NaCl, 1 mM dithiothreitol (DTT),[1] 1 mM EDTA, and 10% glycerol with protease inhibitors (0.1 mM phenylmethylsulfonyl fluoride, 10 μg/mL leupeptin, and 5 μg/mL aprotinin). Clarified extracts were dialyzed against a buffer of 20 mM 2-(4-morpholino)ethanesulfonic acid (pH 6.0), 1 mM EDTA, and 1 mM DTT and then subjected to cation-exchange chromatography on S-Sepharose. The peak of P/CAF activity eluted at 0.6 M NaCl in a 0−0.8 M linear gradient of NaCl. Fractions with HAT activity were pooled and concentrated to a volume of 2−3 mL. Concentrated sample was then dialyzed against G-75 column buffer applied to a G-75 Sephadex size exclusion column and eluted in a buffer of 50 mM Tris (pH 7.5 at 4 °C), 150 mM NaCl, 1 mM DTT, and 10% glycerol. Fractions containing purified P/CAF (assessed by SDS−polyacrylamide gel electrophoresis) were pooled and stored at −20 °C until use. Protein concentrations were determined by the method of Bradford (*18*).

Enzymatic Assays for P/CAF. P/CAF histone acetyltransferase activity was monitored continuously using a Multiskan Ascent microplate reader (LabSystems, Franklin, MA) as previously described (*17*). The CoA generated in the HAT reactions was continuously measured by using a coupled enzyme system of pyruvate dehydrogenase. The CoA-dependent oxidation of pyruvate is accompanied by the reduction of NAD to NADH, which was measured spectrophotometrically at 340 nm. The pyruvate dehydrogenase coupled enzyme has the advantage that AcCoA is regenerated in the coupled reaction (*17*). Thus, AcCoA is concomitantly replenished with every turnover of the enzyme. Stock solutions of the H3 peptide or Ac-Lys-14 H3 peptide were prepared fresh daily (at a final concentration of 1.75 mM) in the presence of 5 mM dithiothreitol (DTT). Alternatively, P/CAF activity was measured using [^{3}H]AcCoA and H3 peptide or calf thymus histones as substrates using a radioactive P81-filter binding assay as described previously (*16*).

pH Profile of the P/CAF-Catalyzed HAT Reaction. At different pH values spanning from 6 to 9.5, the $k_{cat}/K_{m(H3)}$ values were determined at saturating levels of AcCoA (50 μM), while varying H3 peptide (25−400 μM). A 50 mM Tris, 50 mM Bis-Tris, and 100 mM sodium acetate (TBA) buffer was employed to keep the ionic strength constant over the pH range examined. The $k_{cat}/K_{m(H3)}$ values were then determined from a fit to eq 1:

$$v = k_{cat}S/(K_m + S) \quad (1)$$

Once the $k_{cat}/K_{m(H3)}$ values were obtained at the indicated pH, the complete data set was fitted to eq 2 or 3:

$$v = C/(1 + H/K_a) \quad (2)$$

$$v = C/(1 + H/K_a)(1 + H/K_b) \quad (3)$$

where C is the pH-independent value, K_a and K_b are individual ionization constants, and H is the proton concentration.

Bi-Substrate Kinetic Measurements. The Bi-substrate kinetic analysis was performed at AcCoA concentrations spanning from 0.71 to 9.1 μM and H3 peptide concentrations spanning from 50 to 300 μM. The P/CAF HAT activity was monitored via the coupled-enzyme spectrophotometric assay using pyruvate dehydrogenase. The data were fitted to three

possible kinetic mechanisms: the sequential (ternary-complex) mechanism equation (eq 4), the ping-pong (covalent-intermediate) mechanism equation (eq 5), and the equilibrium-ordered equation (eq 6), using the algorithms of Cleland (*25*) and the computer program KinetAsyst (IntelliKinetics, State College, PA), using a nonlinear least-squares approach. In these equations, K_{ma} is the K_m value for A, K_{mb} is the K_m value for B, and K_{ia} is the dissociation constant for A. Also, the dissociation constant for B, K_{ib}, is determined from the relationship $K_{ib} = K_{ia}(K_{mb}/K_{ma})$:

$$v = V_m AB/(K_{ia}K_b + K_{ma}B + K_{mb}A + AB) \quad (4)$$

$$v = V_m AB/(K_a B + K_b A + AB) \quad (5)$$

$$v = V_m AB/(K_a K_b + K_b A + AB) \quad (6)$$

Kinetic Measurements with Inhibitors. CoA and Ac-Lys-14 H3 peptide, products of the P/CAF-catalyzed HAT reaction, were used in steady-state inhibition studies. The data from these studies were fitted to the respective inhibition equations: competitive (eq 7), noncompetitive (eq 8), or uncompetitive (eq 9), based on the algorithms defined by Cleland (*25*) using a nonlinear least-squares analysis.

$$v = V_m S/[K_m(1 + I/K_{is}) + S] \quad (7)$$

$$v = V_m S/[K_m(1 + I/K_{is}) + S(1 + I/K_{ii})] \quad (8)$$

$$v = V_m S/[K_m + S(1 + I/K_{ii})] \quad (9)$$

Synthesis of Bimane-Labeled H3 Peptide. In a typical reaction, approximately 1.0 μmol of H3 peptide in 50 mM Tris, pH 7.5, and 2.5 μmol DTT were mixed with an excess (30 μmol) of monobromobimane at 4 °C. At pH 7.5, the sulfhydryl of the C-terminal cysteine will be preferentially labeled. The reaction was allowed to proceed for 2 h prior to quenching the bimane labeling by adding excess DTT (15 μmol). The bimane-labeled peptide was purified by reversed phase chromatography using a Beckman BioSystem 510 with Ultrasphere column (4.6 mm × 15 cm). Portions of the reaction were loaded in 0.05% trifluoroacetic acid/H_2O for 1 min prior to running a 0−40% acetonitrile linear gradient. Bimane-labeled H3 peptide eluted at 17% acetonitrile while the unmodified H3 peptide eluted at 13% acetonitrile. The bimane-labeled H3 peptide was dried and resuspended in 50 mM Tris, pH 7.5, 5 mM DTT, and the concentration was determined via a spectrophotometric wavelength scan and a extinction coefficient of 6.0 mM^{-1} cm^{-1} at 391 nm. The bimane-labeled H3 peptide was subsequently tested as a substrate for P/CAF and exhibited kinetic parameters identical to unlabeled peptide. In addition, 100% of purified bimane-labeled H3 peptide was viable to acetylation.

Determination of the Dissociation Constant for AcCoA and Bimane-Labeled H3 Peptide via Equilibrium Dialysis. Equilibration was performed using Dispo-Equilibrium Dialyzers (Amika Corp.) which contain two 75 μL chambers separated by a 5 kDa cutoff dialysis membrane. The dialyzers were pretreated with 0.01% BSA. For determination of the dissociation constant for AcCoA, equilibration conditions were 50 mM Tris, 50 mM Bis-Tris, 100 mM sodium acetate, pH 7.5, and 2.5−3.0 μM P/CAF. The K_d value for AcCoA was determined by aliquoting 0.4−10 μM AcCoA (20−40 cpm of [^{3}H]/pmol) into the buffer chamber, and P/CAF into the sample chamber. After 48 h of equilibration on a level shaker, samples were recovered from each chamber and counted by liquid scintillation to determine the amount of radioactivity in the buffer chamber ($[AcCoA]_{free}$) and the sample chamber ($[AcCoA]_{free} + [AcCoA{\cdot}P/CAF]$) in order to determine the amount of bound AcCoA. The data were presented in hyperbolic form and fitted to eq 10:

$$[AcCoA{\cdot}P/CAF] = ([P/CAF]_{tot}[AcCoA]_{free})/(K_d + [AcCoA]_{free}) \quad (10)$$

For determination of the dissociation constant for bimane-labeled H3 peptide, equilibration conditions were 50 mM Tris, pH 7.5, and 50 μM P/CAF in the presence or absence of 50 μM CoA (on each side of the membrane). The K_d value of P/CAF for bimane-labeled H3 peptide in the presence or absence of CoA was determined by aliquoting bimane-labeled H3 peptide (concentrations spanning 15−330 μM) into the buffer/sample chamber, and P/CAF with and without CoA into the sample chamber. After 48 h of equilibration, samples were recovered from each chamber and analyzed by UV−visible absorption spectroscopy. Alternatively, the samples were analyzed by fluorometry with excitation at 393 nm and bimane emission detected at 475 nm. As before, the data were presented in hyperbolic form and fitted to eq 11:

$$[\text{bimane-H3}{\cdot}P/CAF] = ([P/CAF]_{tot}[\text{bimane-H3}]_{free})/(K_d + [\text{bimane-H3}]_{free}) \quad (11)$$

Quench-Flow Analysis. The rate-limiting step was examined using a Hi-Tech quench-flow device (Hi-Tech Ltd., Salisbury, U.K.). P/CAF (∼5 μM) and 50 μM [^{3}H]-acetyl-CoA were rapidly mixed with 400 μM H3 peptide at 22 ± 3 °C, pH 7.5 (concentrations given are post-mixing). At times between 0 and 1.0 s, the reactions were quenched with 2 N HCl, and the amount of [^{3}H]-acetyl-H3 peptide was quantified by spotting 50 μL of the 200 μL reaction slug on P81-phosphocellulose paper and washing away the free AcCoA in sodium bicarbonate buffer. Variations in the dilution of the slug were corrected versus an internal control of total ^{3}H radioactivity. This was done by spotting 50 μL of the reaction slug onto P81-phoshocellulose paper without washing prior to scintillation counting. Control experiments with P/CAF and [^{3}H]-acetyl-CoA quenched prior to the addition of H3 peptide yielded insignificant counts, consistent with the lack of an acetyl-enzyme intermediate being involved in the reaction. Due to a linear increase in product formation and the lack of an apparent burst or lag phase, data were fitted to a linear least-squares analysis.

For the quench-flow analysis under single turnover conditions, ∼5 μM P/CAF and 400 μM H3 were rapidly mixed with 0.5 μM [^{3}H]-acetyl-CoA at 22 ± 3 °C, pH 7.5 (concentrations given are post-mixing). After various reaction times between 0 and 9 s, the reactions were quenched with 2 N HCl, and the amount of [^{3}H]-acetyl-H3 peptide was determined as described above. Data were fitted to a first-order exponential: $[\text{product}] = Ae^{(-kt)} + B$, where A is the amplitude, k is the first-order rate constant, B is the total amount of product, and t is time.

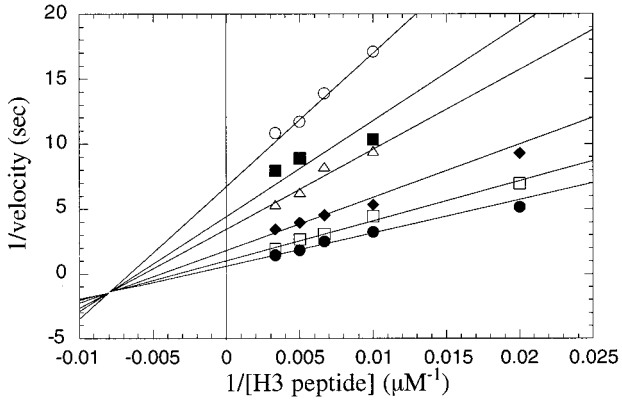

FIGURE 1: Bi-substrate kinetic analysis indicates ternary complex formation between P/CAF, AcCoA, and histone H3 peptide. A plot of 1/velocity versus 1/[H3 peptide] at multiple fixed concentrations of AcCoA. The pyruvate dehydrogenase coupled assay was used to monitor H3 peptide acetylation at pH 7.5, 25 °C. The AcCoA concentrations were as follows: open circles, 0.071 μM; filled squares, 0.11 μM; open triangles, 0.143 μM; filled diamonds, 0.286 μM; open squares, 0.571 μM; filled circles, 1.14 μM. Three additional higher concentrations of AcCoA were used (2.29 μM, 4.6 μM, and 9.2 μM) in fitting, but for clarity they are not displayed. The concentration of P/CAF was 67 nM, and H3 peptide concentration spanned 50−300 μM. Data were fitted to eq 4 for a sequential mechanism (KinetAsyst, Intellikinetics, State College, PA) as described under Experimental Procedures. The experiment was performed in duplicate with one of the double-reciprocal plots displayed.

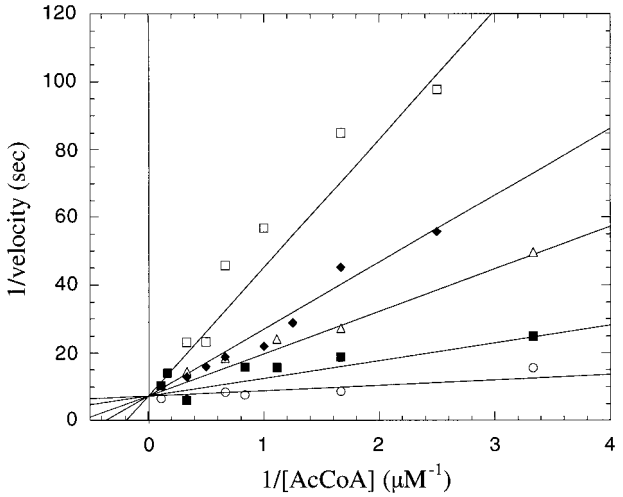

FIGURE 2: CoA is a competitive inhibitor toward AcCoA during P/CAF-catalyzed HAT reaction. The radioactive P81-filter binding assay was used to monitor activity. The data are plotted as 1/velocity versus 1/[AcCoA] at a fixed concentration of 100 μM H3 peptide, and various fixed concentrations of CoA: open circles, 0 μM; filled squares, 1 μM; open triangles, 3 μM; filled diamonds, 5 μM; and open squares, 10 μM. Data were fitted to eq 7 (KinetAsyst, Intellikinetics, State College, PA). The reaction conditions were 50 mM Tris, 50 mM Bis-Tris, 100 mM sodium acetate, pH 7.5, and 100 nM P/CAF at 25 °C and a total reaction volume of 55 μL.

RESULTS

Bi-Substrate Kinetics. Bi-substrate kinetic analyses were carried out to distinguish between a possible sequential, ping-pong, or equilibrium-ordered kinetic mechanism. P/CAF catalyzes the acetyl group transfer from AcCoA to the ϵ-amino group acceptor of lysine-14 within histone H3. Thus, the reaction involves two substrates, AcCoA and H3 histone, and generates two products, CoA and Ac-Lys-14 H3. Because enzyme-catalyzed acetyl group transfer reactions can utilize acetyl-enzyme intermediates (ping-pong) or direct transfer (sequential), it was necessary to perform Bi-substrate steady-state analyses to differentiate among the possible mechanisms. Initial velocities were determined as a function of H3 peptide concentrations and at various fixed concentrations of AcCoA (Figure 1). The data were fitted to either a sequential, a ping-pong, or an equilibrium-ordered kinetic model. The data clearly exhibited a best fit to the simple sequential mechanism. The complete data set in Figure 1 was fitted directly to eq 4, using nonlinear least-squares fitting. Typically, the data are plotted in double-reciprocal form and display an intersecting line pattern which intersects to the left of the $1/v$ axis. The double reciprocal lines displayed in Figure 1 are the theoretical lines that would be predicted based upon the best nonlinear least-squares fit. The sequential model requires that both AcCoA and H3 must bind to form a ternary complex with P/CAF prior to catalysis. Because the intersection point does not lie on the $1/v$ axis, binding of substrates is not in rapid equilibrium (equilibrium-ordered mechanism) during turnover. The average values from two separate experiments yielded a k_{cat} value of 2.3 ± 0.07 s^{-1}. The K_{ia}, K_m, and k_{cat}/K_m values for AcCoA were 0.30 ± 0.12 μM, 0.98 ± 0.31 μM, and 2.3 ± 0.80 × 10^6 M^{-1} s^{-1}, respectively. The K_{ib}, K_m, and k_{cat}/K_m values for H3 peptide were 186 ± 117 μM, 532 ± 81 μM, and 4.3 ± 0.81 × 10^3 M^{-1} s^{-1}, respectively. Although the data clearly indicate the requirement for a ternary complex, the order of substrate addition and product release cannot be established from these experiments alone.

Product Inhibition. To determine the order of substrate binding and product release, product inhibition studies were performed. The authentic reaction products CoA and Ac-Lys-14 H3 peptide were examined as inhibitors of the forward HAT reaction. The type of inhibition (i.e., competitive, uncompetitive, and noncompetitive) of the various substrate/product pairs is diagnostic for a particular kinetic mechanism. In these experiments, one substrate and one product concentration is varied while the other substrate concentration is held constant, and the initial enzymatic rates are measured. The data are fitted to the appropriate equations and displayed in double reciprocal plots. Initially, CoA was examined as an inhibitor versus the substrate AcCoA, at fixed H3 peptide concentrations (Figure 2). CoA exhibited simple competitive inhibition against AcCoA, with an inhibition constant (K_i) of 0.44 ± 0.12 μM. In double reciprocal form, the lines at various fixed concentrations of CoA intersect at the $1/v$ axis, indicating that at high AcCoA concentrations, the CoA can be competed away and the actual k_{cat} of P/CAF can be observed. The lack of an $1/v$ intercept effect indicates that CoA and AcCoA bind to the same form of the enzyme. Given the requirement for a ternary complex (sequential mechanism), this suggests that CoA and AcCoA bind to the free form of the enzyme. By default, AcCoA must be the first substrate to bind P/CAF, and CoA must be the last product released (Scheme 1). Consistent with this kinetic mechanism, inhibition studies of CoA versus H3 produced no significant inhibition when AcCoA was present at saturating levels.

To provide additional evidence for the proposed mechanism of Scheme 1, the product Ac-Lys-14 H3 peptide was examined as a substrate against AcCoA and H3 peptide. As

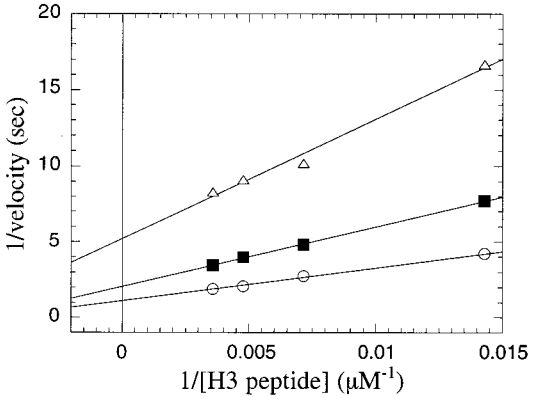

FIGURE 3: Inhibition of P/CAF by the product Ac-Lys-14 H3 peptide when H3 peptide is the varied substrate. Data are presented in double reciprocal form, where $1/v$ is plotted versus 1/[H3 peptide], at various fixed concentrations of Ac-Lys-14 H3 peptide (circles, 0 mM; squares, 1.0 mM; and triangles, 2.0 mM). The [P/CAF] was 70 nM, and [AcCoA] was 65 μM. The reaction conditions were 50 mM Tris, 50 mM Bis-Tris, 100 mM NaOAc, pH 7.5 and 25 °C. Data sets were fitted to a noncompetitive inhibition equation, eq 8 (KinetAsyst, Intellikinetics, State College, PA). The experiments were performed in triplicate with a representative plot displayed.

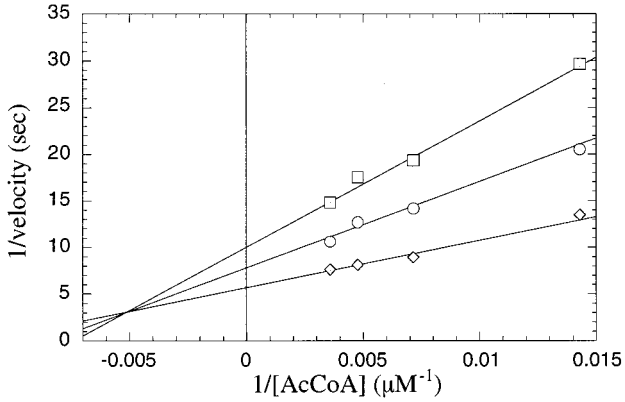

FIGURE 4: Inhibition of P/CAF by the product acetylated H3 (Ac-Lys-14 H3) peptide when AcCoA is the varied substrate**.** Data are presented in double reciprocal form, where $1/v$ is plotted against 1/[AcCoA], at various fixed concentrations of Ac-Lys-14 H3 peptide (diamonds, 0 mM; circles, 1.0 mM; and squares, 2.0 mM). The P/CAF concentration was 70 nM, and [H3 peptide] was 233 μM. The reaction conditions were 50 mM Tris, 50 mM Bis-Tris, 100 mM NaOAc, pH 7.5 and 25 °C. Each data set was fitted to noncompetitive inhibition, eq 8 (KinetAsyst, Intellikinetics, State College, PA). The experiments were performed in triplicate with representative plots displayed.

Scheme 1: Proposed Kinetic Mechanism for P/CAF Histone Acetyltransferase

$$E \underset{k_2}{\overset{k_1 A}{\rightleftharpoons}} EA \underset{k_4}{\overset{k_3 B}{\rightleftharpoons}} EAB \underset{k_6}{\overset{k_5}{\rightleftharpoons}} EPQ \xrightarrow{k_7} EQ \xrightarrow{k_9} E$$

A= acetyl-CoA; B= H3 histone; P= acetyl-H3; Q= CoA.

$$k_{cat}/K_A = k_1 \qquad k_{cat}/K_B = k_3k_5k_7/(k_5k_7 + k_4k_7 + k_4k_6)$$

$$k_{cat} = k_5k_7k_9/(k_9k_7 + k_6k_9 + k_5k_9 + k_5k_7)$$

predicted by the kinetic model, Ac-Lys-14 H3 peptide exhibited noncompetive inhibition versus both H3 peptide (Figure 3) and AcCoA (Figure 4). With H3 as the varied substrate, the K_{is} and K_{ii} values for Ac-Lys-14 H3 peptide were 1.3 ± 0.37 mM and 0.66 ± 0.07 mM, respectively. With AcCoA as the varied substrate, the K_{is} and K_{ii} values for Ac-Lys-14 H3 peptide were 1.1 ± 0.31 mM and 2.5 ± 0.64 mM, respectively. With respect to each substrate binding event, Ac-Lys-14 H3 peptide binds to a distinct form of the enzyme, and there is a reversible connection between the binding of Ac-Lys-14 H3 peptide and each substrate binding event. Collectively, these data strongly support the kinetic model proposed in Scheme 1, where substrate binding and product release are fully ordered.

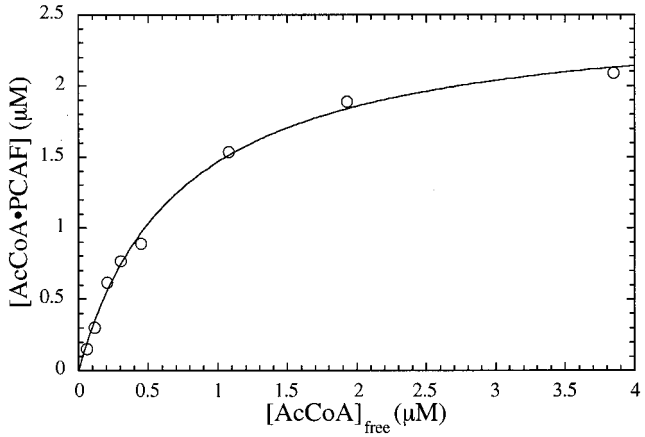

FIGURE 5: Determination of the dissociation constant (K_d) for AcCoA binding to P/CAF via equilibrium dialysis. The data are presented in hyperbolic form, where [AcCoA·P/CAF] is plotted versus $[AcCoA]_{free}$. Equilibration conditions were 50 mM Tris, 50 mM Bis-Tris, 100 mM NaOAc, pH 7.5, and 2.5 μM P/CAF. Equilibration was performed using Dispo-Equilibrium Dialyzers (Amika Corp.) which contains two 75 μL chambers separated by a 5 kDa MW cutoff dialysis membrane. The K_d value for AcCoA in the presence of P/CAF was determined by aliquoting 0.4−10 μM AcCoA (20−40 cpm of $[^3H]$/pmol) into the buffer chamber, and P/CAF into the sample chamber. After equilibration (48 h) on a level shaker, samples were recovered from each chamber and counted by liquid scintillation to determine the amount of radioactivity in the buffer chamber ($[AcCoA]_{free}$) and in the sample chamber ($[AcCoA]_{free}$ + [AcCoA·P/CAF]) in order to determine the amount of bound AcCoA. The data were fitted to: [AcCoA·P/CAF] = $([P/CAF]_0[AcCoA]_{free})/(K_d + [AcCoA]_{free})$. The experiment was performed in duplicate with a representative plot displayed.

Equilibrium Binding Assays. The kinetic model of Scheme 1 predicts that AcCoA will exhibit relatively high-affinity binding for the free form of P/CAF. To determine the affinity of AcCoA binding to free enzyme, equilibrium dialysis was performed in the absence of H3 peptide, and the dissociation constant (K_d) for AcCoA binding to P/CAF was determined. Varying concentrations of $[^3H]$-AcCoA were aliquoted into the buffer chamber, and P/CAF was placed into the sample chamber of the equilibrium dialyzers, separated by a semipermeable membrane (5 kDa MW cutoff). After equilibration, samples were recovered from each chamber and were counted by liquid scintillation. To determine the amount of bound AcCoA, the data were analyzed as described under Experimental Procedures. A representative binding curve is shown in Figure 5. The average value from two separate experiments yielded a K_d value of 0.64 ± 0.12 μM and an estimated enzyme concentration that was only 34% lower (average) than the P/CAF concentration estimated by the method of Bradford (*18*). The good agreement with the expected enzyme concentration provides additional validation of the method and suggests that most (if not all) of the purified P/CAF has adopted the native active conformation. Interestingly, the K_i value (0.44 μM) of CoA obtained from enzyme kinetic methods is very similar to the K_d value of

0.64 μM obtained from equilibrium dialysis. This suggests that the acetyl group of CoA contributes little to the binding energy. Consistent with this, the X-ray structure of the P/CAF·AcCoA complex revealed only a single contact to the acetyl moiety (*14*). Also, the relatively high-affinity binding of AcCoA to free enzyme provides further support for the ordered addition of AcCoA followed by H3 peptide (Scheme 1).

Also, the proposed kinetic model of Scheme 1 predicts that substrate H3 binds more tightly to the AcCoA-bound form of P/CAF than to the free enzyme. To examine this directly, we have performed equilibrium dialysis with a fluorescently labeled H3 peptide. The synthetic H3 peptide (residues 1−20) was engineered to contain a carboxy-terminal cysteine residue (equivalent to position 21). The free cysteine-containing H3 peptide was reacted with mbB to produce the bimane-labeled H3 peptide. The labeled peptide was purified using reverse phase HPLC (Experimental Procedures). To verify that the bimane moiety had no effect on the HAT reaction, this modified peptide was examined as a substrate. The labeled peptide exhibited kinetic parameters that were indistinguishable from those of the parent H3 peptide (data not shown). Varying concentrations of bimane-labeled H3 were aliquoted into the buffer chamber, and a fixed concentration of P/CAF was placed into the sample chamber of the equilibrium dialyzers. In two separate experiments, CoA was either included or excluded in the equilibrium dialysis. CoA was employed instead of AcCoA because AcCoA would be turned over by the enzyme in the presence of the acceptor peptide, obfuscating the analysis. As we have shown, the acetyl group provides little additional binding enhancement. After equilibration, samples were recovered from each chamber, and the concentration of labeled peptide on each side was quantified by both absorbance and fluorescent measurements. The amount of H3 peptide bound was determined and plotted as a function of free H3 peptide. In the absence of CoA, no discernible amount of H3 peptide binding (up to 330 μM) was observed (Figure 6). In dramatic contrast, when CoA was included at 50 μM (~100-fold greater than the K_d), efficient H3 binding was detected. The concentration of bound peptide was plotted against free peptide, and the data were fitted to eq 11, yielding a K_d of 116 ± 17 μM and an effective enzyme concentration of 39 ± 2.9 μM. The K_d value of 116 μM is in excellent agreement with the value of 186 ± 117 μM obtained from the Bi-substrate kinetic experiments (Figure 1). Consistent with our proposed model, H3 peptide binds to P/CAF only after CoA/AcCoA has bound.

pH Dependence of P/CAF HAT Activity. To establish the critical ionizations for the P/CAF reaction, the steady-state parameter k_{cat}/K_m for H3 peptide was determined as a function of pH value. These experiments were performed at saturating AcCoA so that any observed ionizations will reflect those required for H3 peptide binding and catalysis. The k_{cat}/K_m constant is an apparent second-order rate constant for the reaction of free peptide with enzyme. Using Scheme 1 as the kinetic model, the k_{cat}/K_m is equal to $k_3k_5k_7/(k_5k_7 + k_4k_7 + k_4k_6)$. Given the thermodynamically unfavorable back-reaction, k_6, the expression can be simplified to $k_3k_5/(k_4 + k_5)$. Thus, the pH dependency of k_{cat}/K_m will reflect important ionizations in H3 peptide binding (k_3) and in chemical catalysis (k_5). At various pH values between 6 and 9.5, individual saturation curves were generated by determining the initial velocities at varying concentrations of H3 peptide, and the k_{cat}/K_m values were calculated from fits to eq 1. In cases where it became difficult to saturate the enzyme with H3 peptide, the slope of the line from an initial rate versus [H3 peptide] plot was determined as the k_{cat}/K_m value. This was necessary at the two pH extremes. Ensuring that saturating levels of AcCoA were employed at the pH extremes (pH 6 and 9.5), higher (50, 100, and 150 μM) concentrations of AcCoA produced no significant increase in the observed rate of catalysis.

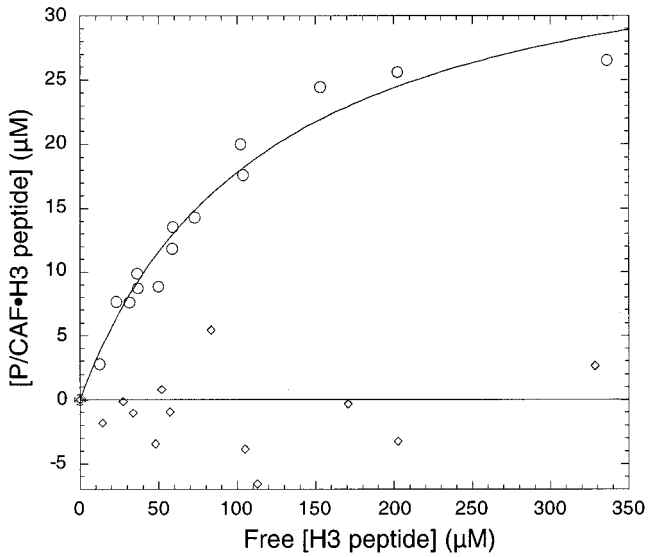

FIGURE 6: Determination of the apparent dissociation constant (K_d) for H3 peptide binding to P/CAF via equilibrium dialysis. The data are presented in hyperbolic form, where [P/CAF·H3 peptide] is plotted versus [H3 peptide]$_{free}$. Equilibration conditions were 50 mM Tris, pH 7.5, and 50 μM P/CAF. Equilibration was performed using equilibrium dialyzers containing two 75 μL chambers separated by a 5 kDa MW cutoff dialysis membrane. The apparent K_d for the binding of H3 peptide by P/CAF was determined in the presence of CoA (open circles) and in the absence of CoA (open diamonds) by aliquoting equal-molar concentrations of CoA (50 and 0 μM, respectively) and bimane-labeled H3 peptide (ranging from 15 to 330 μM) into both the buffer and sample chambers, and P/CAF into the sample chamber. After equilibration (40 h), samples were recovered and analyzed by UV−visible absorption spectroscopy (ϵ_{390} = 6 mM^{-1} cm^{-1}), and/or bimane fluorescence versus a standard curve of bimane-labeled-H3 peptide, to determine the amount of bimane-labeled H3 peptide in the buffer chamber ([H3 peptide]$_{free}$) and in the sample chamber ([H3 peptide]$_{free}$ + [P/CAF·H3 peptide]). The amount of bound H3 peptide was subsequently ascertained from the raw data. The data were fitted to: [P/CAF·H3 peptide] = ([P/CAF]$_0$[H3 peptide]$_{free}$)/(K_d + [H3 peptide]$_{free}$). The experiment was performed in duplicate with the combined data plotted.

The resulting pH profile (Figure 7) clearly displayed two ionizations that must be unprotonated for activity. Fitting the data to eq 3 yielded pK_a values of 6.9 ± 0.25 and 7.5 ± 0.22, and a pH-independent value of (7.2 ± 0.74) × 10^3 M^{-1} s^{-1}. Because the k_{cat}/K_m value reflects both binding and catalysis, the observed ionizations can result from either enzyme or H3 peptide or both. However, the H3 peptide ARTKQTARKSTGGKAPPKQL employed in these reactions does not harbor ionizable groups that would be in the range 6.6−7.7 for those ionizations observed in Figure 7. Thus, these two important ionizable groups likely reside on P/CAF. Similarly, the pH dependence of the k_{cat} value, which

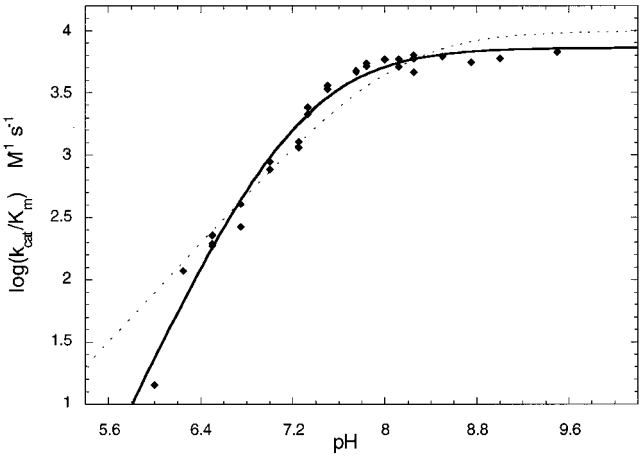

FIGURE 7: k_{cat}/K_m pH profile of P/CAF HAT activity. At the indicated pH values, the k_{cat}/K_m value was determined as described under Experimental Procedures. The coupled enzyme spectrophotometric assay was employed between pH 6.5 and 9.25, and the radioactive P81 filter binding assay was used at pH 6−6.25 and pH 8.25−9.5. The solid line is a fit to eq 3, while the dashed line is a fit to eq 2.

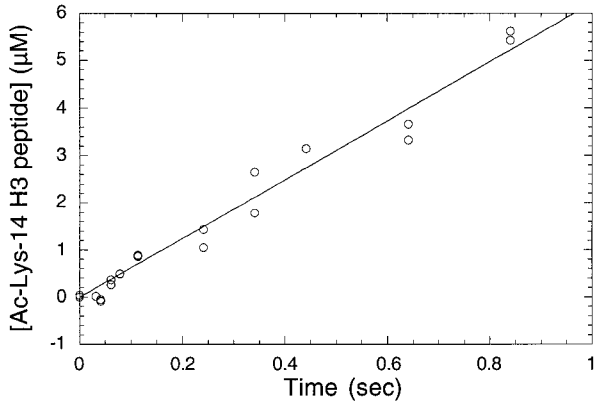

FIGURE 8: Determination of the rate-limiting step via quench-flow analysis under multiple turnover conditions. Using a Hi-Tech quench-flow device, ~5 μM P/CAF and 50 μM [^{3}H]-acetyl-CoA were rapidly mixed with 400 μM H3 peptide at 22 ± 3 °C, pH 8 (concentrations given are post-mixing). After various reaction times between 0 and 1 s, the reactions were quenched with 2 N HCl, and the amount of [^{3}H]-acetyl-H3 peptide was determined using the filter binding assay (Experimental Procedures). Data were fitted to a linear least-squares fit to determine the turnover rate. The experiment was performed in quadruplet with a representative plot displayed.

was determined in the pH range 6.5−8.3, displayed an ionization with a pK_a value of 8.19 ± 0.24 that must be unprotonated for activity, and a pH-independent value of 12 ± 5 s^{-1} (data not shown). Because of the greater uncertainty in k_{cat} values at the pH extremes, we could not unequivocally rule out the existence of a second unprotonated group below a pK_a value of ~6.6, or of a required protonated group with pK_a greater than ~9.

To fully interpret pH profiles and to propose roles for the identified ionizations, the nature of the rate-limiting step should be established; otherwise erroneous assignments could be made. As discussed above, according to our proposed model (Scheme 1), the k_{cat}/K_m for peptide will reflect H3 binding (k_3) and chemical catalysis (k_5). The k_{cat} value will reflect chemical catalysis (k_5), release of Ac-Lys-14 H3 (k_7), and release of CoA (k_9), according to $k_{cat} = k_5k_7k_9/(k_9k_7 + k_6k_9 + k_5k_9 + k_5k_7)$ (Scheme 1). This equation simplifies to $k_5k_7k_9/(k_9k_7 + k_5k_9 + k_5k_7)$, if k_6 is small as expected. Moreover, because turnover is often controlled by a single slow step, the k_{cat} expression will likely simplify to a single rate constant (either k_5, k_7, or k_9).

Rapid Reaction Kinetics. To establish the rate-limiting step in turnover, rapid reaction kinetic experiments were carried out using a quench-flow apparatus. These pre-steady-state kinetic experiments should help distinguish among rate-limiting (i) H3 peptide binding, k_3; (ii) chemical catalysis, k_5; and (iii) product release, k_7 or k_9. Given these models, three distinct kinetic product curves are possible under multiple turnover conditions. If H3 peptide binding is rate-limiting in turnover, the kinetic trace should display a significant lag phase followed by a linear phase. If chemistry is rate-limiting, the kinetic trace will be linear, even at the very early stages of the reaction. If a product release step is rate-determining, then the trace should display an exponential burst of product, followed by a slower linear phase. In all cases, the linear phase should correspond to the steady-state initial velocity. Under single turnover conditions (i.e., [P/CAF] > [substrate]), the first-order exponential rate of Ac-Lys-14 H3 peptide formation will provide the rate of chemistry when substrate binding is not a slow step. Thus, if k_{cat} agrees with the first-order rate obtained in the single turnover experiment, then chemistry is rate-limiting.

In multiple turnover experiments, P/CAF was rapidly reacted with H3 peptide at saturating levels of [^{3}H]-AcCoA. At various times, the reaction was quenched with HCl, and the amount of [^{3}H] transferred to H3 peptide was quantified. The amount of product formed was then plotted against time (Figure 8). Over a time range of 10 ms to 1 s, the data produced a linear curve that passed through the origin. No apparent pre-steady-state burst or lag was discernible from the kinetic traces. The data of Figure 8 are a representative data set of four separate experiments performed at pH 7.5 and 8. Within experimental error, the rate constant (1.2 ± 0.1 s^{-1}, pH 8) determined from the slope of the lines was entirely consistent with rate constants obtained from separate steady-state kinetic assays (1.2 ± 0.4 s^{-1}, pH 8). These data strongly suggest that peptide binding (k_3 in Scheme 1) and product release steps (k_7 and k_9) do not limit the rate of the overall reaction. Instead, the rate of acetyl group transfer ($k_{cat} \sim k_5$) appeared to limit the rate of catalysis.

To provide further evidence for rate-limiting chemistry, a single turnover experiment was performed (Figure 9). P/CAF (5 μM) and H3 peptide (400 μM) were rapidly mixed with a substoichiometric amount of AcCoA (0.5 μM), and the formation of acetyl-H3 was determined as before. The progress curved yielded a first-order exponential with a rate constant of 1.6 ± 0.3 s^{-1}. The steady-state turnover rate under these conditions yielded a value of 0.9 ± 0.2 s^{-1}. The good agreement between these values provides additional evidence that chemistry (k_5) limits catalytic turnover.

DISCUSSION

The steady-state kinetic data provided in these studies strongly support a completely ordered Bi-Bi sequential mechanism (Scheme 1). A ternary complex is formed in a sequential manner, with AcCoA binding first followed by histone H3 peptide. In the ternary complex, the ϵ-amino group of Lys-14 directly attacks the carbonyl of AcCoA,

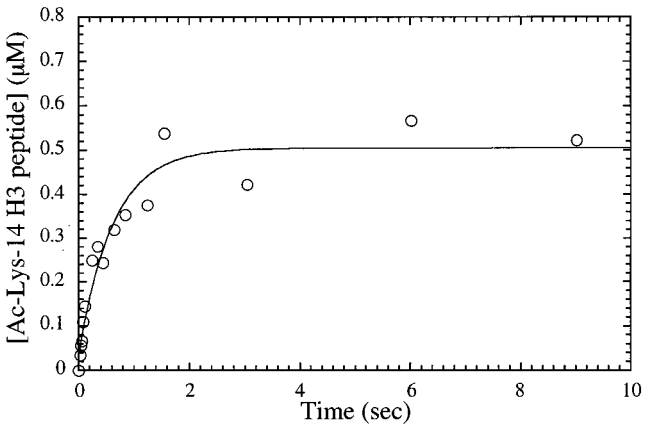

FIGURE 9: Determination of the rate of chemistry via quench-flow analysis under single turnover conditions. Using a Hi-Tech quench-flow device, ~5 μM P/CAF and 400 μM H3 were rapidly mixed with 0.5 μM [^{3}H]-acetyl-CoA at 22 ± 3 °C, pH 7.5 (concentrations given are post-mixing). After various reaction times between 0 and 9 s, the reactions were quenched with 2 N HCl, and the amount of [^{3}H]-acetyl-H3 peptide was determined using the filter binding assay as described under Experimental Procedures. Data were fitted to a first-order exponential: [product] = $Ae^{(-kt)} + B$ where A is the amplitude, k is the first-order rate constant, B is the total amount of product, and t is time. The experiment was performed in duplicate with a representative plot displayed.

transferring the acetyl moiety to the acceptor peptide. Products are released in an ordered fashion, where Ac-Lys14 H3 is the first and CoA is the last product released. Corroborating evidence for the substrate binding order was provided by the equilibrium dialysis experiments. The model predicts that free P/CAF would display relatively high-affinity binding for AcCoA compared to H3 peptide. Moreover, the mechanism suggests that P/CAF can bind H3 peptide only after AcCoA is bound. These predictions were experimentally verified by equilibrium binding experiments. AcCoA binds to free P/CAF with a K_d value of 0.6 μM, while H3 peptide exhibited no detectable binding to free enzyme. However in the presence of saturating CoA, H3 binding was readily observed, resulting in a K_d value of 116 μM. Given the similar binding affinities between CoA (K_d = 0.4 μM) and AcCoA (K_d =0.6 μM), we would suggest that the dissociation constant for peptide binding to the [P/CAF·CoA] complex may accurately reflect the true dissociation constant for peptide binding to the substrate·enzyme complex, [P/CAF·AcCoA]. This conclusion is consistent with structural evidence which indicated that the interactions of the pyrophosphate group and pantetheine arm of CoA (in the *Tetrahymena* GCN5·CoA·H3 peptide ternary complex) are nearly superimposable with the interactions observed in the binary *Tetrahymena* GCN5·AcCoA complex (*15*, *19*).

Consistent with our biochemical data, the NMR (*19*) and X-ray structures (*15*) of the *Tetrahymena* GCN5 HAT bound to both CoA and an H3 peptide revealed that, indeed, CoA and peptide bind to separate hydrophobic grooves along the surface of the enzyme. Although, a ternary complex of P/CAF has not been solved, the recent structure of the CoA·P/CAF binary complex revealed similar substrate binding pockets (*14*). Our data suggest that CoA or AcCoA binding will induce conformational movements within the H3 binding pocket which will facilitate higher affinity binding of H3 peptide. This is supported by the structural changes observed between free enzyme, CoA-bound enzyme, and a ternary enzyme·CoA·H3 peptide complex (*14*, *15*, *19*, *20*). Upon CoA binding, the enzyme undergoes a conformational change within the C-terminal β5-turn−α4 and α5-turn−β6 protein segments. These movements widen both substrate binding grooves. In the *Tetrahymena* GCN5·CoA·H3 peptide structure, the widening of the substrate grooves was even more pronounced (*15*).

The quench-flow experiments strongly suggested that chemical catalysis (k_5 in Scheme 1) limits the turnover rate of the enzyme at pH 7.5−8.0. There was good agreement between steady-state and rapid reaction (quench-flow) observed rates. No burst or lag in acetyl-H3 product formation was discernible. This was a significant finding, since experimental perturbations of enzyme activity, such as pH effects, will reflect changes in the rate of chemistry and will provide insight into how chemical catalysis is accomplished.

The pH dependence for the k_{cat}/K_m value revealed two enzyme ionizations (pK_a values of 6.9 and 7.5) that must be unprotonated for P/CAF activity (binding/catalysis). For the related yeast GCN5 HAT, we had observed previously an ionization (pK_a ~8) that must be unprotonated for both k_{cat} and k_{cat}/K_m constants when calf thymus histones were employed as substrate (*16*). In that study, we demonstrated that the ionization with a pK_a of ~8 was Glu-173. We proposed that Glu-173 was the general base in the HAT reaction, abstracting a proton from the ϵ-amino group of lysine and facilitating the direct nucleophilic attack of lysine on the carbonyl carbon of bound AcCoA (*16*). Because this residue is conserved between human P/CAF and yeast GCN5, the group with a pK_a of 7.5 in P/CAF may be the equivalent glutamic acid (Glu-570 in P/CAF). In the solved X-ray structures of P/CAF and GCN5, this conserved glutamic acid is found at the intersection point between two hydrophobic troughs (*14*, *15*), consistent with its proposed role as a general base (*16*).

The better assay precision encountered when using the H3 (residues 1−20) synthetic peptide has allowed us to uncover a second ionizable group with a pK_a value of 6.9. Because the k_{cat}/K_m is a measure of both peptide binding and catalysis, this ionization could be critical for either binding or catalysis. Also, since chemical catalysis is slow, the observed pK_a values are not predicted to be kinetically perturbed and are likely to be close to their intrinsic values. The synthetic peptide (ARTKQTARKSTGGKAPPKQLC) harbors no groups whose pK_a values would be ~6.9. Thus, this group will reside within the enzyme. Although pK_a values can be physically altered within the enzyme environment, we analyzed the solved P/CAF and GCN5 structures for the presence of a conserved histidine residue that occupies either the active site or the two substrate binding grooves. We identified His-543 (P/CAF) within the H3 peptide binding pocket as the potential critical residue. In the *Tetrahymena* GCN5 ternary complex structure, Asp-91 was hydrogen-bonded to the equivalent histidine (His-94) via the ND1 nitrogen. These two conserved residues form a critical loop structure between α-helix 2 and β-strand 2. Helix 2 forms one side of the hydrophobic wall within the peptide binding groove. In addition to the van der Waals interactions of this helix with bound peptide, Tyr-84 was hydrogen-bonded to the substrate backbone carbonyl of residue 10. The NE2 imidazolium nitrogen of His-94 was pointed in toward the side chain of Ser-10 from the bound H3 peptide. Unfortu-

nately, the electron density of the peptide in this region was poor, and the molecular model was constructed using an alanine at this position. We have modeled in a serine side chain and shown that the NE2 nitrogen of His-94 and the side chain oxygen of substrate Ser-10 can position themselves to less than 3 Å (data not shown), suggestive of a possible hydrogen bonding interaction. For this stabilizing interaction, the histidine must be unprotonated, consistent with the required unprotonated ionization ($pK_a = 6.9$) observed in the k_{cat}/K_m pH profile for peptide binding/catalysis. Furthermore, we have previously demonstrated that a conserved arginine residue (Arg-164 in yeast GCN5), proximal to the histidine, was playing a direct role in binding the phosphate group from the Ser-10 phosphorylated H3 peptide (*21*). Future mutational studies will be required to establish whether His-543 is a critical residue in peptide substrate binding.

In a related study, we have recently characterized the yeast HAT enzyme, GCN5 (*22*). Interestingly, human P/CAF and yeast GCN5 display similar catalytic turnover rates and k_{cat}/K_m values for H3 peptide, suggesting a common catalytic mechanism and a common mode of H3 peptide binding. However, P/CAF exhibits >10-fold higher affinity for CoA and AcCoA than GCN5. Since no structural data exist on the yeast GCN5·CoA complex, we cannot comment on the physical basis for this difference, but the biological implications of such a difference may be dramatic. Since mammals harbor both GCN5 and P/CAF, the relative efficiency of these HATs to acetylate Lys-14 of H3 will depend, in part, upon the available concentration of AcCoA. For instance, at [AcCoA] below ~0.8 μM, P/CAF will acetylate H3 ~10-fold faster than GCN5. At [AcCoA] > ~8 μM, the enzymes will be similarly active. The difference in binding affinity also suggests that GCN5 activity could respond more dramatically to changes in cellular [AcCoA]. Moreover, the fact that the binding affinities between substrate AcCoA and product CoA are similar (with respect to each enzyme) predicts that cellular ratios of AcCoA/CoA (*23*, *24*) would be a critical determinant for in vivo HAT activity. This important feature may link HAT-dependent transcriptional activation/repression activity with various cellular and metabolic pathways.

ACKNOWLEDGMENT

We thank C. David Allis for providing the P/CAF expression vector and Ronen Marmorstein for providing the X-ray coordinates.

REFERENCES

1. Neuwald, A. F., and Landsman, D. (1997) *Trends Biochem. Sci. 22* (5), 154−155.
2. Yang, X. J., Ogryzko, V. V., Nishikawa, J., Howard, B. H., and Nakatani, Y. (1996) *Nature 382* (6589), 319−324.
3. Mizzen, C. A., and Allis, C. D. (1998) *Cell Mol. Life Sci. 54* (1), 6−20.
4. Kouzarides, T. (1999) *Curr. Opin. Genet. Dev. 9*, 40−48.
5. Ogryzko, V. V., Schiltz, R. L., Russanova, V., Howard, B. H., and Nakatani, Y. (1996) *Cell 87* (5), 953−959.
6. Bannister, A. J., and Kouzarides, T. (1996) *Nature 384* (6610), 641−643.
7. Schiltz, R. L., Mizzen, C. A., Vassilev, A., Cook, R. G., Allis, C. D., and Nakatani, Y. (1999) *J. Biol. Chem. 274* (3), 1189−1192.
8. Sartorelli, V., Puri, P. L., Hamamori, Y., Ogryzko, V., Chung, G., Nakatani, Y., Wang, J. Y., and Kedes, L. (1999) *Mol. Cell 4* (5), 725−734.
9. Herrera, J. E., Sakaguchi, K., Bergel, M., Trieschmann, L., Nakatani, Y., and Bustin, M. (1999) *Mol. Cell. Biol. 19* (5), 3466−3473.
10. Liu, L., Scolnick, D. M., Trievel, R. C., Zhang, H. B., Marmorstein, R., Halazonetis, T. D., and Berger, S. L. (1999) *Mol. Cell. Biol. 19* (2), 1202−1209.
11. Xu, W., Edmondson, D. G., and Roth, S. Y. (1998) *Mol. Cell. Biol. 18* (10), 5659−5669.
12. Dhalluin, C., Carlson, J. E., Zeng, L., He, C., Aggarwal, A. K., and Zhou, M. M. (1999) *Nature 399* (6735), 491−496.
13. Brownell, J. E., Zhou, J., Ranalli, T., Kobayashi, R., Edmondson, D. G., Roth, S. Y., and Allis, C. D. (1996) *Cell 84* (6), 843−851.
14. Clements, A., Rojas, J. R., Trievel, R. C., Wang, L., Berger, S. L., and Marmorstein, R. (1999) *EMBO J. 18* (13), 3521−3532.
15. Rojas, J. R., Trievel, R. C., Zhou, J., Mo, Y., Li, X., Berger, S. L., Allis, C. D., and Marmorstein, R. (1999) *Nature 401*, 93−98.
16. Tanner, K. G., Trievel, R. C., Kuo, M.-H., Howard, R., Berger, S. L., Allis, C. D., Marmorstein, R., and Denu, J. M. (1999) *J. Biol. Chem. 274*, 18157−18160.
17. Kim, Y., Tanner, K. G., and Denu, J. M. (2000) *Anal. Biochem. 280* (2), 308−314.
18. Bradford, M. M. (1976) *Anal. Biochem 72*, 248−254.
19. Lin, Y., Fletcher, C. M., Zhou, J., Allis, C. D., and Wagner, G. (1999) *Nature 400* (6739), 86−89.
20. Trievel, R. C., Rojas, J. R., Sterner, D. E., Venkataramani, R. N., Wang, L., Zhou, J., Allis, C. D., Berger, S. L., and Marmorstein, R. (1999) *Proc. Natl. Acad. Sci. U.S.A. 96* (16), 8931−8936.
21. Cheung, P., Tanner, K. G., Cheung, W. L., Sassone-Corsi, P., Denu, J. M., and Allis, C. D. (2000) *Mol. Cell 5*, 905−915.
22. Tanner, K. G., Langer, M. R., and Denu J. M. (2000) *J. Biol. Chem. 275*, 22048−22055.
23. Reibel, D. K., Wyse, B. W., Berkich, D. A., and Neely, J. R. (1981) *Am. J. Physiol. 240*, H606−H611.
24. Rock, C. O., Calder, R. B., Karim, M. A., and Jackowski, S., (2000) *J. Biol. Chem. 275*, 1377−1383.
25. Cleland, W. W. (1977) *Adv. Enzymol. Relat. Areas Mol. Biol. 45*, 273−387.

BI001272H